Improvement in Predicting Stand Growth of *Pinus radiata* (D. Don) across Landscapes Using NOAA AVHRR and Landsat MSS Imagery Combined with a Forest Growth Process Model (3-PGS)

Nicholas Coops

Abstract

Recent detailed physiological and micro-meteorological studies of forest ecosystems have lead to new insights that greatly simplify the prediction of gross primary production (P_G) and above-ground net primary production (NPP_A) which are key variables related to conventional measures of forest growth, such as mean annual increment (MAI) of stemwood. These simplifications were applied in a monthly time-step model (Physiological Principles Predicting Growth using Satellite data (3-PGS)) which requires monthly weather data (average minimum and maximum temperatures and precipitation), an estimate of soil texture, rooting depth, and the fraction of photosythetically active radiation absorbed by the forest canopies (fPAR) which is estimated from a satellite-derived normalized difference vegetation index (NDVI).

The model was originally tested at sites in Australia and New Zealand using coarse spatial resolution AVHRR Pathfinder data which effectively limited the predictions of NPP_A to broad areas. In this paper, AVHRR and Landsat MSS data are both used by the model, allowing 3-PGS predictions to be applied at a more refined landscape scale.

Accumulated above ground biomass predicted by the model was compared with biomass data from discrete stands in a 2,265-ha Pinus radiata *(D. Don) plantation in southern New South Wales, Australia. There was a linear relation between predicted and measured wood production ($r^2 = 0.84$). Additionally, analysis of the results indicated the incorporation of MSS and AVHRR data allowed a variety of stand-specific disturbances to be accounted for, such as thinning.*

Introduction

Over the past 10 to 15 years, a number of models designed to predict forest productivity on the basis of physiological processes have been developed. The models deal with processes at leaf (Nilson and Ross, 1997), canopy (Martin and Aber, 1996), plot (Comins and McMurtrie, 1993), regional (FOREST-BGC; Running and Coughlan, (1988)), and global (Prince and Goward, 1995) scales. To date, most of these models have only been used as research tools, and their calculation of forest growth is complicated, involving detailed, multi-variable relations requiring a great deal of information and careful parameterization. A recently developed model (3-PG, Physiological Principles Predicting Growth) (Landsberg and Waring, 1997) utilizes a number of simple but soundly based relationships derived from earlier research which allow process-based calculations to be combined with allometric and other empirical relationships to produce estimates of forest growth in terms of a few variables, such as diameter at breast height (DBH), leaf area index (LAI), and basal area (BA).

Coops *et al.* (1998) modified the original 3-PG model to allow it to be driven by remotely sensed observations. The modified model, called 3-PGS (the S symbolizing the use of satellite data in the model framework), uses a monthly time step and requires values for monthly minimum and maximum temperature, total monthly rainfall, soil water storage capacity, an estimate of soil fertility, and the fraction of photosythetically active radiation absorbed by the forest canopies (*f*PAR) which is estimated from a satellite-derived index, based on the normalized difference between reflectances measured in the near-infrared and red wavelengths, termed the normalized difference vegetation index (NDVI).

In the original application of the 3-PGS model, the coarse spatial resolution AVHRR data effectively limited the predictions of NPP_A and total NPP to large areas. While this was deemed adequate for global or continental analysis (Goward and Dye, 1996), it obviously limited the application of the results at more refined landscape scales. By combining fine spatial resolution Landsat Multispectral Scanner (MSS) data (80-m pixel size) with 8- by 8-km Advanced Very High Resolution Radiometer (AVHRR) Pathfinder data, it should be possible to dis-aggregate the 3-PGS predictions within each AVHRR pixel and re-distribute forest productivity estimates at finer scales. The higher spatial resolution MSS imagery should allow, at the very least, basic discrimination of forest age classes while maintaining monthly NDVI (and, thus, *f*PAR) estimates from the AVHRR dataset.

The objective of this paper is to test the 3-PGS model at a landscape scale using the two sets of remotely sensed data. As a result of difficulties in obtaining accurate forest growth information in native Australian forests, growth was predicted for a *Pinus radiata* (D. Don) plantation in southern

CSIRO Forestry and Forest Products, Private Bag 10, Clayton South MDC, Victoria 3169, Australia (N.Coops@ffp.csiro.au).

Photogrammetric Engineering & Remote Sensing, Vol. 65, No. 10, October 1999, pp. 1149–1156.

0099-1112/99/6510–1149$3.00/0

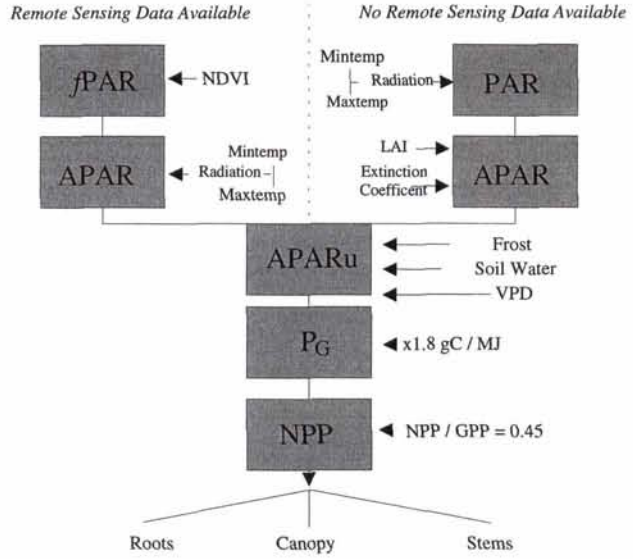

Figure 1. Diagrammatic flow of components of the 3-PGS model. APAR = Absorbed Photosynthetically Active Radiation, APARu = Utilizable APAR, P_G = Gross Primary Productivity, NPP = Net Primary Productivity, NPP_A = above-ground NPP, NDVI = Normalized Difference Vegetation Index.

New South Wales (N.S.W.) for which extensive forest growth information was available.

Description of the Stand Growth Model (3-PG)

The 3-PG model was developed by Landsberg and Waring (1997) as a simple process-based model. Absorbed photosynthetically active radiation (APAR) is estimated from global solar radiation derived, if necessary, from an established empirical relationship based on average maximum and minimum temperatures. The utilized portion of APAR (APARu) is obtained by reducing APAR by an amount determined by a series of modifiers derived from constraints imposed by (1) stomatal closure, caused by high day-time atmospheric VPD's (see Landsberg and Waring, 1997); (2) soil water balance, which is the difference between total monthly rainfall, plus available soil water stored from the previous month, and transpiration, calculated using the Penman-Monteith equation with canopy conductance modified by LAI of the forest and constrained by monthly estimates of VPDs (reaching a maximum value of 0.02 ms^{-1}) (Kelliher *et al.*, 1995); and (3) the effects of sub-freezing temperatures (< 0°C) using a frost modifier calculated from the number of frost days per month. The modifiers take values between 0 (system "shutdown") and 1 (no constraint) (see Landsberg, 1986; McMurtrie *et al.*, 1994; Runyon *et al.*, 1994). Gross primary production (P_G) is calculated by multiplying APARu by a constant canopy quantum efficiency coefficient (α, assumed in this study to be 1.8 g C MJ^{-1}; see Landsberg and Waring (1997)). A major simplification in the 3-PG model is that it does not require calculation of respiration or root turnover, but rather assumes that total net primary production (NPP) in temperate forests approximates a fixed fraction (0.45 $\pm$ 0.05) of P_G (Landsberg and Waring, 1997; Waring *et al.*, 1998). LAI determines radiation interception and photosynthesis, and foliage biomass is calculated from measured or derived values of specific leaf area (Pierce *et al.*, 1994), and is updated at the end of each month as a balance between new growth of foliage and fixed (or variable rates) of leaf litterfall. The model partitions NPP into root and above-ground foliage and stem mass. The fraction of total NPP allocated to root growth increases from 0.2 to 0.6 as the ratio APARu/APAR decreases from 1.0 to 0.2.

Structure of the Stand Model with Satellite Inputs (3-PGS)

In 3-PGS, the fraction of photosythetically active radiation absorbed by the forest canopies (*f*PAR) is estimated from a satellite-derived NDVI. This spectral vegetation index has been shown, both empirically and theoretically, to be related to the *f*PAR absorbed by vegetation canopies (Kumar and Monteith, 1982; Sellers, 1985; Sellers, 1987; Goward *et al.*, 1994). Despite several possible limitations to such an inference (such as the effect of topographic shadowing and understory effects), NDVI appears to be a good approximation to *f*PAR absorbed by canopies, integrated over the diurnal cycle (Prince and Goward, 1995).

Coops *et al.* (1998) utilized 3-PGS to predict above-ground NPP (NPP_A) at eight contrasting forested sites in Australia and New Zealand and compared them with estimated NPP_A derived from field data. Data from the Pathfinder dataset (Agbu and James, 1994) provided monthly estimates of landscape greenness derived from near-infrared and red reflectances, which are closely related to the *f*PAR that is absorbed by vegetation. Although the analysis was limited to a single year (1987), there was a linear relation between NPP_A predicted by the model and on-the-ground estimates of wood production (usually > 75 percent of NPP_A) for (potentially) fully stocked, rapidly growing stands (r^2 = 0.82). The analysis also provided an assessment of the relative importance of climatic variables upon production.

The 3-PGS model can be summarized as a series of procedural steps (see Figure 1) as follows:

(1) Estimates of total incoming radiation are derived from temperature data (Bristow and Campbell, 1984), if not directly available. PAR was assumed to be 0.5 of total incoming solar radiation and APAR was partitioned by (a) multiplying PAR by *f*PAR if satellite data was available or (b) applying Beer's law with modeled LAI estimates (using an extinction coefficient of 0.5 (Landsberg and Waring, 1997)).
(2) If frost occurs, APAR is reduced in proportion to the days per month below freezing.
(3) Soil water balance is calculated as the difference between precipitation, storage capacity of the soil, and water transpired by or evaporated from the vegetation, carrying stored soil water forward from month to month. The soil water modifier is based on the ratio of currently available to soil water capacity.
(4) The VPD modifier is calculated for each month from average values of VPD. (Either the soil water, frost, or the VPD modifier applies — whichever is the most severe in any month).
(5) Monthly PG is calculated by multiplying APARu by α.
(6) NPP is calculated as 0.45 x P_G.
(7) The ratio APARu/APAR determines the fraction of NPP allocated to roots, with the remainder available for above-ground growth.

The Project

Tallanganda *Pinus radiata* plantation is located adjacent to Tallanganda State Forest (35° 30'S; 149° 30'E) in southeastern Australia. The State Forest covers over 56,000 ha and is predominantly composed of native eucalypt species. The soil in the region is sandy clay loam to sandy clay (State Forests N.S.W., 1995), and the maximum water storage capacity of the plantation was estimated on the basis of soil series information (Australian Society of Soil Science, 1985) and was set to 150 mm. The elevation of the site is 1100 m with a climate characterized by warm summers, cool to cold winters, and relatively uniform monthly rainfall. Annual rainfall is between 600 and 700 mm with an average summer tempera-

ture range between 23 and 29°C while winter average temperatures range from 7 to 13°C (State Forests of N.S.W., 1995).

Site Data

A *P. radiata* plantation was established in 1968 after clearance of approximately 100 ha of native forest. The initial spacing was at 3 by 3 m (1200 stems per hectare). The plantation was subsequently increased by planting additional stands at irregular intervals until 1982. Current plantation size is 2,265 ha, comprising 50 stands in nine individual age classes. Figure 2 shows the distribution of the age classes within the plantation.

Forest Growth Data

The plantation has been measured at irregular intervals since its establishment. The most recent inventories were undertaken in 1992 and 1997 when 15 of the 50 stands were measured. This involved the establishment of randomly located plot or plots within each age class. In 1997, seven of the nine age classes were measured with basal area (BA), stand density, and stand height data collected to provide an estimate of mean DBH for each plot. Standing volume was calculated by applying a cylindrical taper coefficient of 0.38 (Knott, 1995). Similar data were available for the two remaining age classes measured in 1992; these data were included to provide a complete dataset. Table 1 summarizes all mensurational data collected at the site.

Satellite Data

AVHRR Pathfinder Data

The AVHRR data were extracted from the Land Pathfinder data set (Agbu and James, 1994) which produces global composites of key variables such as the NDVI, surface temperature estimates, and albedo surfaces from July 1981 to August 1994. Due to the small geographic extent of the plantation, a single NDVI value (representing an 8- by 8-km area) was extracted from the monthly AVHRR Pathfinder dataset for each month from 1982 to 1994. Based on studies of Holben (1986) and Goward *et al.* (1994), the raw NDVI values as obtained from the Pathfinder dataset were re-scaled. This was required because the satellite NDVI measurements are consistently lower than near-surface (ultralight aircraft) observations, indicative of atmospheric attenuation. As a result, a simple linear adjustment was preformed on the NDVI values to ensure that they were comparable with the values used by Goward *et al.* (1994).

The adjustment is of the form

$$NDVI_{surface} = (1.1 * NDVI_{satellite}) + 0.11.$$

To predict *f*PAR from NDVI, we used the equation developed by Goward *et al.* (1994): i.e.,

$$\text{Fraction of PAR absorbed (\%)} = (121 * NDVI_{surface}) - 4.0$$

where $NDVI_{surface}$ is the atmospherically corrected NDVI from the Pathfinder dataset.

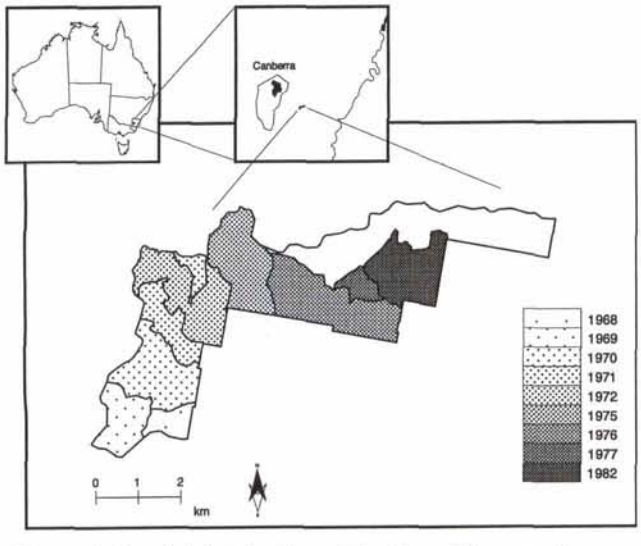

Figure 2. Spatial distribution of the *P. radiata* age classes at Tallanganda State Forest.

TABLE 1. SUMMARIZED *P. RADIATA* PLOT INVENTORY DATA FROM TALLANGANDA PINE PLANTATION.

Age Class	Density (stems/ha)	Basal Area (m^2/ha)	Height (m)	Wood Volume (m^3/ha)	Above-Ground Biomass of Stems (tons/ha)
1968	564	43.0	31.0	400	159.9
1969	402	32.8	29.0	285	114.1
1970	503	40.0	30.8	369	147.8
1971	539	42.5	29.2	372	148.8
1972	671	42.1	29.3	370	147.9
1975	709	37.9	24.2	275	109.8
1976	877	44.2	22.6	300	120.0
1977	911	37.7	21.0	238	95.0
1982	602	14.2	13.0	55	22.2

Landsat MSS

Remotely sensed data in the near-infrared and red regions of the electromagnetic spectrum have been available at a landscape scale since the launch of Landsat 1 in 1972. To take advantage of the historical databases from the MSS available in Australia, a number of images were analyzed (Table 2). Image processing involved two stages: (1) geometric and atmospheric correction and (2) derivation of NDVI for each age class stand.

All MSS images were geometrically referenced, using a nearest-neighbor routine, to the Australian Map Grid (AMG) using 1:25,000-scale base maps of the area with a root-mean-square (RMS) error of less than 80 meters for all processed images. The digital numbers (DNs) recorded by the MSS were converted to physical values of radiance (Price, 1987) so that meaningful comparisons could be made between images recorded on different scanners and dates (Lee and Marsh, 1995). Atmospheric correction involved the suppression of

TABLE 2. DETAILS OF THE LANDSAT MSS IMAGES USED IN THIS STUDY.

Landsat	Date	Path	Row[a]	Image Center Latitude (°:')	Image Center Longitude (°:')
1	01/Nov/72	95	85	S36:01	E150:32
2	28/Aug/80	95	NS	S35:30	E150:33
4	12/Sep/82	90	85	S35:49	E149:24
4	13/Jul/83	90	85	S36:05	E149.20
5	07/Jul/84	90	85	S35:50	E149:25
5	24/Jun/85	90	85	S35:49	E:149:28
5	11/Aug/85	90	85	S35:50	E149:27
5	19/Feb/86	90	85	S35:49	E149:30
5	18/Sep/87	90	85	S35:49	E149:26
5	25/Feb/88	90	85	S35:28	E149:35

[a] NS Indicates Non-Standard scene center

TABLE 3. SUMMARY OF CLIMATIC DATA FOR TALLANGANDA PINE PLANTATION IN 1987.

	Jan	Feb	Mar	Apr	May	Jun	Jul	Aug	Sep	Oct	Nov	Dec
Maxtemp (°C)	23.7	21.6	18.7	14.9	11.5	9.5	10.3	13.3	17.3	20.6	23.1	24.2
Mintemp (°C)	16.7	11.6	10.0	7.4	5.4	4.2	4.0	4.6	5.9	7.3	9.0	11.4
Rainfall (mm)	72	60	55	63	60	58	50	62	58	72	70	58
Average Daily Radiation ($MJ\ m^{-2}\ day^{-1}$)	24.1	20.6	19.6	17.4	14.4	12.9	13.9	16.9	20.6	23.4	25.7	26.2
Vapour Pressure Deficit (kPa)	22.0	20.0	16.9	13.1	9.3	7.4	7.2	8.2	10.1	12.2	15.6	19.7
Frost Days	0	0	0	3	11	17	20	16	10	3	1	0

the effect of atmospheric scattering using the modified dark object subtraction technique of Chavez (1988). To suppress irradiance differences between images, a method similar to that of Curran *et al.* (1992) was adopted. The July 1983 image was chosen as the standard for normalizing the other images. This choice was based on the fact that the July 1983 image exhibited the least offset of lowest DN values between bands and the greatest dynamic range of values throughout the image. The mean radiance of objects assumed to be unchanging (such as deep water and sand) was compared between the July 1983 image and all others. The difference in each spectral band was then used to normalize the other images by subtracting the difference between the mean radiances and the atmospherically corrected radiances in all other images.

The mean NDVI (using the 600- to 700- and 800- to 1100-nm channels of Landsat MSS) was calculated for each of the 50 stands in the plantation, using boundary information provided by State Forests of N.S.W. Pixels located along boundaries between stands, roads, and creeks were not used in the calculation of NDVI to ensure that the values were as uncontaminated by non-forest pixels as possible. A mean NDVI value was also computed from the MSS imagery for the 8- by 8-km area of the AVHRR Pathfinder pixel. This was used to normalize the MSS NDVI values to the regional AVHRR NDVI value which was required because the AVHRR NDVI estimate was a composite of daily AVHRR estimate (Holben, 1986) and the Landsat MSS NDVI data were a single snapshot.

The normalization of the MSS NDVI values to comparitive AVHRR NDVI estimates was of the form

$$NDVI_{scaled\ MSS} = NDVI_{actual\ MSS} * (NDVI_{8\text{- by }8\text{-km MSS}}/NDVI_{AVHRR\ satellite}).$$

To predict *f*PAR from the scaled MSS NDVI values, the same equation developed by Goward *et al.* (1994) for the Pathfinder data was used.

Meteorological Data

The 3-PGS model required monthly estaimtes of rainfall, minimum and maximum temperature, the number of days when frost occurred, and total incoming solar radiation. Data from an automatic meteorological station within the plantation provided daily measurements of rainfall which were summed to monthly means. Temperature and frost records were not available locally so mean monthly temperature estimates were derived for the plantation using the ESOCLIM package (Hutchinson, 1984). These monthly estimates were then scaled by actual meteorological conditions as recorded by the nearest climate station (Canberra Airport) to provide estimates of actual monthly climatic data for the simulations. The number of frost days for each month were taken directly from the Canberra Airport meteorological station. Incoming solar radiation was not recorded at the site, so total incoming solar radiation was calculated from empirical relationships (Goldberg *et al.*, 1979) using a technique first developed by Bristow and Campbell (1984) and later incorporated into a more general model by Hungerford *et al.* (1989). This procedure relates diurnal air temperature amplitude to atmospheric transmittance and has been shown to predict incoming solar radiation with over 90 percent accuracy and an average standard error of 1.0 $MJ\ m^{-2}day^{-1}$ (Coops *et al.*, 1998).

The climatic conditions of the study area for 1987 are given in Table 3.

Simulations

The model was run, following the procedure outlined above, from January 1968 to January 1997. To allow the variation within each age class to be estimated, the model was simulated for all stands in the plantation ($n = 50$); however, only 15 of the stands predictions could be compared to the available inventory data. Initial stem, foliage, and root mass were selected to represent one-year-old pine seedlings, and the initial number of stems was set to the initial planting density. Root turn over (0.015 percent per month), litter fall (0.02 percent per month), and specific leaf area (6.0 m^2/kg) were set the same as specified by Landsberg and Waring (1997). For months where AVHRR Pathfinder data were available (January 1982 through December 1994) AVHRR NDVI was used to partition *f*PAR. For other months, *f*PAR was estimated using Beer's law from monthly simulations of canopy LAI (Landsberg and Waring, 1997).

Ten Landsat MSS scenes were available for the analysis; however, only six images coincided with the AVHRR Pathfinder data. If, during the simulation, an MSS scene was available, the following procedure was followed. From each MSS image, mean NDVI was calculated for each of the 50 stands and a mean MSS NDVI value was computed for the equivalent area of the 8- by 8-km AVHRR pixel. The mean MSS NDVI for each stand was then re-scaled using the ratio of the AVHRR NDVI pixel with the mean MSS NDVI value for the same area.

Normalizing the mean MSS NDVI response for each stand to the AVHRR NDVI value was required because the MSS NDVI response is an instantaneous NDVI value captured at the time of overpass of the Landsat satellite. The AVHRR NDVI estimate is a composite value derived from comparing a number of NDVI scenes. As a result, an NDVI value from the MSS data cannot be expected to equal the AVHRR NDVI for the same area. Normalizing ensured that the MSS NDVI values remained consistent with the monthly AVHRR NDVI estimates as well as allowing the use of the Prince and Goward (1995) conversion to *f*PAR.

*f*PAR for each stand ($n = 50$) was then calculated using the scaled MSS NDVI value, and an estimate of P_G for each stand was predicted by 3-PGS using environmental data and the physiological modifiers for that respective month. This value was compared with the predicted P_G of the stand based on climatic and AVHRR data alone. The ratio of these two values provided a scaling factor by which the future monthly P_G allocation to the stand could be increased or decreased. The scaling factor was of the form

$$\text{Scaling factor for each stand} = P_{G\ AVHRR\ computed}/P_{G\ MSS\ computed}.$$

As a result, if the 8- by 8-km AVHRR NDVI value was the same as the mean MSS NDVI value for a single stand, the scaling factor would be 1, indicating no change was required in

the future allocation of P_G to that stand. Scaling factors of less than 1 indicated that the broad-scale AVHRR-derived estimate of P_G, when applied to the stand, was in excess. As a result, the allocation of biomass to that stand would be reduced, using the MSS derived P_G as a fine-scale indication of the stands *f*PAR capacity. Conversely, in stands where the scaling factor was greater than 1, the allocation of biomass would be increased.

This scaling factor was used continually to adjust the monthly P_G allocated to the stand until either (1) a subsequent MSS scene provided a new scaling factor or (2) the end of the AVHRR Pathfinder dataset was reached.

Results

Figure 3 shows the mean MSS NDVI values from 1972 to 1988 averaged for each age class. This figure demonstrates the relationship between NDVI and light absorbing capacity of the different age classes. Plantation planting commenced in 1968, with large sections of the native eucalypt forest being cleared for plantings during the following 5 years. As a result, the 1972 scene indicates that most of the stands had very low NDVI values (in some cases less than 0.1). The second Landsat MSS scene (acquired in August 1980) showed significant cover changes in many of the stands since 1972, with the 1968-1975 stands all having significantly increased NDVI values. In contrast, the 1982 age class produced a high NDVI response in 1980 but the NDVI response fell by the time the next MSS scene was acquired in 1982 because the native forest had been cleared ready for plantation establishment. By 1984, all pine plantation planting was complete and all age classes were growing, producing mean NDVI responses of 0.2 or greater. Figure 3 indicates a relationship between age class and the magnitude of the NDVI, with the older age classes all producing higher NDVI values with lower values typical of younger age classes (such as the 1982 age class). This general trend is expected, given the relatively young age of the forest, with most stands still actively accumulating a canopy. We would expect a cross-over of NDVI trajectories when the growth of the younger stands surpasses that of the older stands when the older canopies become more open again.

The 3-PGS predicted accumulation of above ground biomass in 1997 averaged for each of the nine *Pinus radiata* age classes is shown in Figure 4. The predictions indicate that, as expected, the older age classes contain the most biomass. The variance markers within Figure 4 provide an indication of the added sensitivity introduced through the use of fine resolution remotely sensed data. If the predictions had been solely based on a physiological model driven only by average weather conditions, differences between stands of the same age class would not have been identified. Figure 4 indicates that there is variation within all age classes (except 1977 planting, where only one stand was established), with the most significant variation occurring within the 1969 age class, with a 4 percent variation in estimated accumulation of above-ground biomass among stands.

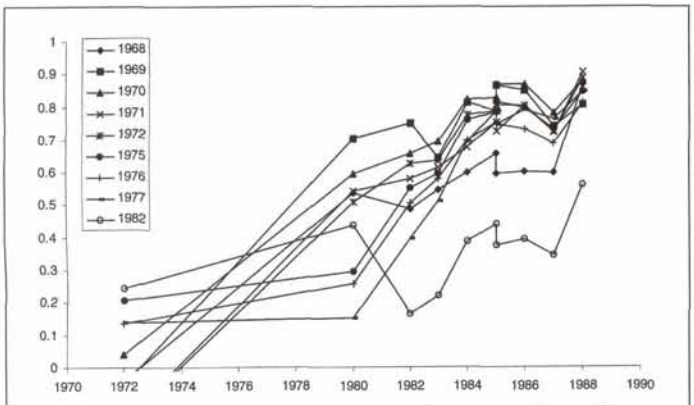

Figure 3. Landsat MSS NDVI values of the nine *P. radiata* age classes from 1972 to 1988.

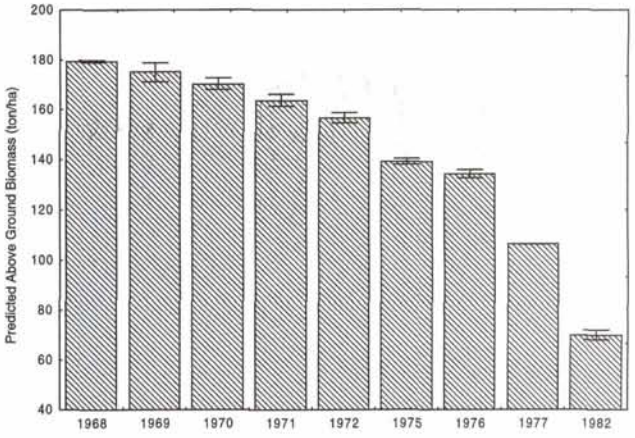

Figure 4. 3-PGS predictions of *P. radiata* standing biomass (tons/ha) for each age class in January 1997. Whiskers indicate within-age class (stand) variation.

Figure 5 shows the effect of introducing fine scale remotely sensing data into the modeling framework. The graph presents the scaling factors, as described earlier, which re-scale the allocation of P_G based on the mean NDVI response for each stand at each time-step where there was an MSS image. This ratio was calculated throughout the simulation when both Pathfinder AVHRR and MSS imagery were available (1982–1994).

Figure 6 shows good agreement ($r^2 = 0.84$) between estimated above-ground accumulation of biomass calculated with 3-PGS and above-ground biomass obtained from the 15 stands in 1992 and 1997. For the stands measured in 1992, simulation results were extracted for year 24 (1992) and used in this comparison.

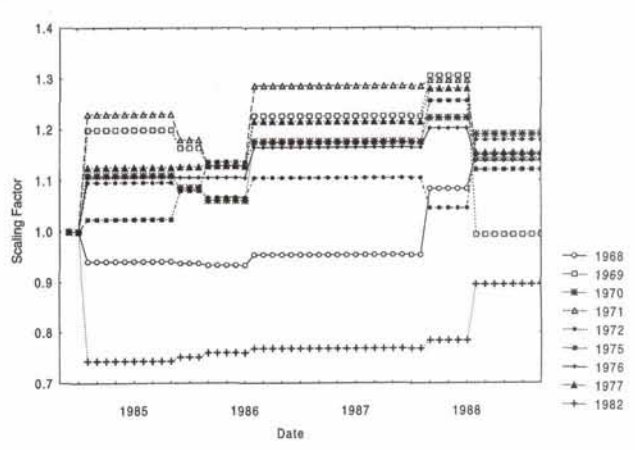

Figure 5. Scaling factors which were used to re-scale the allocation of P_G based on the mean NDVI response of the MSS and the AVHRR pixel for each stand. This ratio was calculated when both AVHRR and MSS imagery were available (1982-1994) and is averaged by age class.

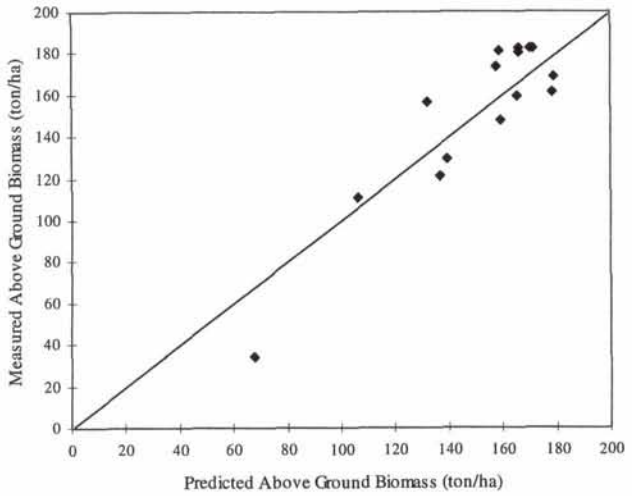

Figure 6. Relationship between 3-PGS predicted above-ground biomass (tons/ha) and actual above-ground stem biomass as derived from field mensuration data.

Discussion

In this paper the incorporation of AVHRR data in the analysis provides monthly estimates of NDVI to predict *f*PAR while periodic MSS data allow assessment of forest age class and thinning regimes for 50 separate stands.

Results indicate that incorporating fine-scale remote sensing data into the analysis can have a significant effect when predicting NPP_A, with the scaling factors ranging from 0.7 to 1.4 (Figure 5). Interestingly, the effect of the scaling appears to be relatively consistent throughout the simulation period for many of the age classes. For example, the 1982 and 1969 age classes have scaling ratios less than 1 throughout the simulation, indicating that estimates of the monthly biomass assigned to these stands were consistently too large based on the AVHRR data alone. The allocation of biomass to these stands was reduced by the inclusion of fine scale remote sensing data. Conversely, stands in the 1969 and 1977 age class grew consistently more rapidly than the physiological model driven by coarse scale AVHRR data alone would predict and, as a result, the age classes were predicted to have more above-ground biomass than otherwise.

Accumulated above-ground biomass predicted by 3-PGS compared well with on-the-ground measurements. Although there was generally good agreement between measured and predicted values, we would not expect these two sets of data to match exactly because of (1) variations in the sampling schemes and (2) distinguishing pine from other vegetation. These issues are discussed below.

First, the ground sampling was restricted to plot-based estimates of above-ground biomass for each age class. This restrictive sampling prevents within-stand variation being estimated. In contrast, 3-PGS predictions were compiled on a raster grid over the entire stand, providing up to 100 cell-based predictions of accumulated biomass for each stand.

Second, the NDVI provides an estimate of the total fraction of radiant energy absorbed by all vegetation in the observed cell, which includes both overstory and understory plants. Any estimate of NPP derived from satellite analyses thus represents the potential photosynthetic capacity of all vegetation, not just the pine forest. This can be a significant factor in Australian native forest environments where the LAI of the overstorey canopy is much lower than pine (Landsberg and Gower, 1997). Likewise, in younger *P. radiata* plantations, NDVI estimates can be biased not just because understorey vegetation is present but also because bare soil can confound interpretation of the NDVI signal. The slight over-prediction of above-ground biomass for the youngest stands at Tallanganda suggests that under-sampling on the ground is most likely a larger contributor than artifacts associated with the NDVI.

Combining remotely sensed data with a process-based growth model brings significant benefits to resource managers whose interest lies at the landscape level of analysis. The benefits of incorporating remotely sensed observations include:

- Detailed records of thinning are not required. The incorporation of remotely sensed data into the simulation model accounts for events such as fire, wind-throw, insect infestations, and thinning which affect stand productivity. This information is difficult to acquire yet essential for landscape-scale growth models, including 3-PG.
- Fine resolution remotely sensed data identified overstocked stands planted in 1968 which had stagnated in growth and canopy development. Subsequently, the field-measured above-ground biomass in these stands was lower than would normally be expected. Calculations of growth from process-based models would normally expect self thinning to have occurred (such as in 3-PG) and, as a result, biomass accumulation rates, from conventional models, would be over-predicted. The inclusion of fine scale remote sensing imagery has resulted in the predicted biomass being reduced to match more closely the field-measured result.
- Remote sensing allows process-based models to be spatially extrapolated across landscapes. In this project 50 individual stands were modeled, with the output of the simulations allowing results to be displayed as growth curves for each stand and as a map of predicted accumulation of above-ground biomass.

We must remember, however, that the MSS NDVI responses within each stand were averaged. As a result, variation occurring within the stands has been ignored. In future work there would be benefits in modeling forest growth on a pixel-by-pixel basis to allow within-stand variation to be accounted for and to provide spatial estimates of forest growth within each stand. Finer resolution modeling of the forest would also allow changes in vegetation composition within stands to be taken more into account. This is particularly the case in those *P. radiata* plantations where buffer strips of natural vegetation are maintained through the plantations to avoid erosion and to provide corridors for native wildlife. While these regions were not used in the computation of the mean NDVI for each age class in this study, the finer resolution model would allow them to be separately modeled and monitored.

Finer resolution application of the model would also allow additional topographic variation to be incorporated into the model inputs. Currently, the remotely sensed data are the only variables which give spatial context to the model. Running simulations over 100-m or finer cells would allow a number of additional topographic variables, such as slope and aspect, to be utilized in the simulation. Fine resolution digital terrain models (DTM) would also provide additional information on soil depth, water holding capacity, and fertility which would allow within-stand variations in productivity to be predicted (McKenzie *et al.*, 1996).

There are some key areas where the satellite data, the modeling procedure, and the use of field data for development and validation can be improved:

- Using currently available MSS satellite data, this study has demonstrated that landscape studies can be undertaken using the 3-PGS methodology. The coarse spatial resolution of the AVHRR Pathfinder dataset still means that less than optimal monthly AVHRR data are being used, providing estimates on the order of an 8- by 8-km spatial resolution. Ideally, full resolution Local Area Coverage (LAC) AVHRR data should be acquired; however, this data archive is not currently available

over the Australian continent for extended periods, thereby limiting its usefulness. In the longer term, launch of the Earth Observation System (EOS), scheduled for the year 2000, will provide data from a new sensor (MODerate resolution Imaging Spectro-radiometer, MODIS) with a near nadir spatial resolution of 250 m, will allow weekly 1 km spatial resolution estimates of net photosynthesis at the global scale (Running *et al.*, 1994).

- The 3-PGS model uses a monthly time step, which has some disadvantages for modeling the water balance of forests. Improvements could be made by introducing a daily time-step version of the model, although this would require significantly more meteorological information (particularly rainfall) at each site, as well as a more accurate estimate of rooting depth of the species, and would lose some of the advantages of the simplified formulation of these models.
- The comparison of model output with actual forest growth information again highlights differences in the way managers and landscape modelers measure the forest. Typically, forest managers in Australia measure tree DBH or basal area of the forest stand in plots. This provides conventional inventory information, but these data are difficult to utilize for biomass estimation because they do not usually include estimates of forest age, height, or composition, or these estimates are poor. In the case of the Tallanganda plantation, where these variables are obviously known, it is still difficult to use inventory data to analyze and utilize in a comparison with above-ground growth estimates for a forest. Forest plantation inventory plots seldom allow the spatial variation within pine stands or age classes to be evaluated, because they assume stands and often age classes to be homogeneous, and as a result, any changes in predictions within, or between, stands of the same age class are difficult to verify.

Conclusions

The application of the 3-PGS model at a landscape scale using remotely sensed data demonstrates a mechanism for extending expensive forest growth plot data over complex terrain and over a variety of stand conditions. The approach allows past management decisions, such as thinning that effect forest productivity but cannot be realistically included in ground-based surveys or simple growth models, to be accounted for. The general correspondence between predicted values of above-ground biomass obtained using 3-PGS, and observed estimates of accumulated biomass from conventional forestry, indicates that the model with satellite-derived information provides a sound framework for regional extrapolation.

Acknowledgments

Dr. Joe Landsberg (CSIRO Land and Water) and Prof. Richard Waring (Oregon State University) developed the original 3-PG framework and contributed greatly to the development of the 3-PGS version of the model. I thank them for their advice and valuable discussions on this project. Drs. Sam Goward, Philip Ryan, and Steve Running and Mr. Ian Mullen provided useful discussions in the development of the model. Mr. Mark Edwards (District Forester, State Forests of N.S.W.) provided growth data and access to Tallanganda Plantation. Mr. Paul Walker and Garry Delbridge provided essential advice and software development in the implementation of the model. Drs. Joe Landsberg, Philip Ryan, Dick Waring and Mr. Ian Mullen read and commented on drafts of this manuscript. I also acknowledge the advice and comments of the two anonymous reviewers. This research was undertaken within CSIRO Multi-Divisional Project 31 on the Spatial Prediction of Forest Productivity. Additional information on this research is available at **http://www.ffp.csiro.au/nfm/mdp/**

References

Agbu, P.A., and M.E. James, 1994. *The NOAA/NASA Pathfinder AVHRR Land Data Set Users Manual*, Goddard Distributed Active Archive Center, NASA Goddard Space Flight Center, Greenbelt, Maryland, xxx p.

Australian Society of Soil Science Inc., Queensland Branch, 1985. *Identification of Soils and Interpretation of Data*, Australian Society of Soil Science Inc., Queensland Branch, Brisbane, Australia, vii + 251 p.

Bristow, K.L., and G.S. Campbell, 1984. On the relationship between oncoming solar radiation and daily maximum and minimum temperature, *Agricultural and Forest Meteorology*, 31:159–166.

Chavez, P.S., 1988. An improved dark-object subtraction technique for atmospheric scattering correction of multi-spectral data, *Remote Sensing of Environment*, 55:1289–1294.

Coops, N.C., R.H. Waring, and J.J. Landsberg, 1998. Assessing forest productivity in Australia and New Zealand using a physiologically-based model driven with averaged monthly weather data and satellite derived estimates of canopy photosynthetic capacity, *Forest Ecology and Management*, 104:113–127.

Comins, H.N., and R.E. McMurtrie, 1993. Long-term response of nutrient-limited forests to CO_2 enrichment: Equilibrium behavior of plant-soil models, *Ecological Applications*, 3:666–681.

Curran, P.J., J.L. Dungan, and H.L. Gholz, 1992. Seasonal LAI in slash pine estimated with Landsat TM, *Remote Sensing of Environment*, 39:3–13.

Goldberg, B., W.H. Klein, and R.D. McCartney, 1979. A comparison of some simple models used to predict solar irradiance on a horizontal surface, *Solar Energy*, 23:81–83.

Goward, S.N., and D.G. Dye, 1996. Global biospheric monitoring with remote sensing, *The Use of Remote Sensing in the Modeling of Forest Productivity* (H.L. Gholz, K. Nakane, and H. Shimoda, editors), Kluwer Academic Publishers, Dordrecht, The Netherlands, pp. 241–272.

Goward S.N., R.H. Waring, D.G. Dye, and J. Yang, 1994. Ecological remote sensing at OTTER: Satellite macroscale observations, *Ecological Applications*, 4:322–343.

Holben, B.N., 1986. Characteristics of maximum value composite images from temporal AVHRR data, *International Journal of Remote Sensing*, 11:1417–1434.

Hungerford, R.D., R.R. Nemani, S.W. Running, and J.C. Coughlan, 1989. *MTCLIM: A Mountain Microclimate Simulation Model*, United States Department of Agriculture Research Paper INT0414, United States Dept. of Agriculture. Ogden, Utah, 52 p.

Hutchinson, M.F., 1984. *A Summary of Some Surface Fitting and Contouring Programs for Noisy Data*, Consulting Report No. ACT 84/6, CSIRO Division of Mathematics and Statistics, CSIRO, Canberra, Australia.

Kelliher, F.M., R. Leaning, M.R. Raupach, and E.D. Schulze, 1995. Maximum conductance for evaporation from global vegetation types, *Agricultural and Forest Meteorology*, 73:1–16.

Knott, J., 1995. *White Cypress Pine Thinning Trials of the Western Region*, Research Paper 27, Research Division, State Forests of NSW, Sydney, Australia, 187 p.

Kumar, M., and J.L. Monteith, 1982. Remote sensing of plant growth, *Plants and the Daylight Spectrum* (H. Smith, editor), Academic Press, London, pp. 133–144.

Landsberg, J.J., 1986. *Physiological Ecology of Forest Production*, Academic Press, Sydney, Australia, 198 p.

Landsberg, J.J., and S.T. Gower, 1997. *Application of Physiological Ecology to Forest Management*, Academic Press, San Diego, California, 354 p.

Landsberg, J.J., and R.H. Waring, 1997. A generalised model of forest productivity using simplified concepts of radiation-use efficiency, carbon balance, and partitioning, *Forest Ecology and Management*, 95:209–228.

Lee, C.T., and S.E. Marsh, 1995. The use of archival Landsat MSS and ancillary data in a GIS environment to map historical change in an urban riparian habitat, *Photogrammetric Engineering & Remote Sensing*, 61:999–1008 .

Martin, M.E., and J.D. Aber, 1996. Estimating forest canopy characteristics as inputs for models of forest carbon exchange by high spectral resolution remote sensing, *The Use of Remote Sensing in the Modeling of Forest Productivity* (H.L. Gholz, K. Nakane,

and H. Shimoda, editors), Kluwer Academic Publishers, Dordrecht, The Netherlands, pp. 61–72.

McKenzie, H.J., P.E. Gessler, P.J. Ryan, and D. O'Connell, 1996. The role of terrain analysis in soil mapping, *Terrain Analysis Workshop* (J.P. Wilson and J. Gallant, editors), NCGIA, Santa Barbara, California.

McMurtrie, R.E., H.L. Gholz, S. Linder, and S.T. Gower, 1994. Climatic factors controlling the productivity of pine stands: A model-based analysis, *Ecological Bulletins*, 43:173–188.

Nilson, T., and J. Ross, 1997. Modeling radiative transfer through forest canopies: Implications for canopy photosynthesis and remote sensing, *The Use of Remote Sensing in the Modeling of Forest Productivity* (H.L. Gholz, K. Nakane, and H. Shimoda, editors), Kluwer Academic Publishers, Dordrecht, The Netherlands, pp. 23–60.

Pierce, L.L., S.W. Running, and J. Walker, 1994. Regional scale relationships of leaf area index to specific leaf area and leaf nitrogen contents, *Ecological Applications*, 4:313–321.

Price, J.C., 1987. Calibration of satellite radiometers and the comparison of vegetation indices, *Remote Sensing of Environment*, 21: 15–27.

Prince, S.D., and S.M. Goward, 1995. Global primary production: A remote sensing approach, *Journal of Biogeography*, 22:815–35.

Running, S.W., and J.C. Coughlan, 1988. A general model of forest ecosystem processes for regional applications. I. Hydrologic balance, canopy gas exchange and primary production processes, *Ecological Modelling*, 42:125–154.

Running, S.W., C.O. Justice, V. Salomonson, D. Hall, J. Barker, Y.J. Kaufmann, A.H. Strahler, A.R. Huete, J.-P. Muller, V. Vanderbilt, Z.M. Wan, P. Teillet, and D. Carneggie, 1994. Terrestrial remote sensing science and algorithms planned for EOS/MODIS, *International Journal of Remote Sensing*, 15:3587–3620.

Runyon, J., R.H. Waring, S.N. Goward, and J.M. Welles, 1994. Environmental limits on net primary production and light-use efficiency across the Oregon transect, *Ecological Applications*, 4: 226–237.

Sellers, P.J., 1985. Canopy reflectance, photosynthesis and transpiration, *International Journal of Remote Sensing*, 68:1335–1372.

———, 1987. Canopy Reflectance, Photosynthesis, and Transpiration 2. The role of Biophysics in the Linearity of Their Interdependence, *Remote Sensing of Environment*, 21:143–183.

State Forests of N.S.W., 1995. *Queanbeyan and Badja Management Areas: Proposed Forestry Operations*, EIS Main Report, Forestry Commission of N.S.W., Pennant Hills, N.S.W., Australia.

Waring, R.H., J.J. Landsberg, and M. Williams, 1998. Net primary production of forests: a constant fraction of gross primary production? *Tree Physiology*, 18:129–134.

(Received 22 October 1997; revised and accepted 24 November 1998)